5-1-2020

Constitutive compressive behavior of polyurea with exposure to aggressive marine environments

Irine Neba Mforsoh
University of Rhode Island

James LeBlanc
Naval Undersea Warfare Center Division Newport

Arun Shukla
University of Rhode Island

Citation/Publisher Attribution

Neba Mforsoh, Irine, James LeBlanc, and Arun Shukla. "Constitutive compressive behavior of polyurea with exposure to aggressive marine environments." *Polymer Testing* 85, (2020). doi: 10.1016/j.polymertesting.2020.106450.

Constitutive compressive behavior of polyurea with exposure to aggressive marine environments

Keywords

Aggressive marine environment; Constitutive behavior; Long term exposure; Polyurea

Polymer Testing 85 (2020) 106450

Contents lists available at ScienceDirect

Polymer Testing

journal homepage: http://www.elsevier.com/locate/polytest

Material Behaviour

Constitutive compressive behavior of polyurea with exposure to aggressive marine environments

Irine Neba Mforsoh [a], James LeBlanc [b], Arun Shukla [a,*]

[a] Department of Mechanical, Industrial and Systems Engineering, University of Rhode Island, Kingston, RI, 02881, USA
[b] Naval Undersea Warfare Center (Division Newport), Newport, RI, 02841, USA

ARTICLE INFO

Keywords:
Polyurea
Aggressive marine environment
Long term exposure
Constitutive behavior

ABSTRACT

The constitutive behavior of polyurea after prolonged exposure to aggressive marine environments, including saline water, UV radiation and combinations of both, was investigated in this study. A diffusion study was performed at several temperatures to determine the effect of temperature on saline water ingression into the polyurea using Crank's method. This diffusion data coupled with Arrhenius' methodology allowed for the calculation of an acceleration factor relating laboratory exposure time at elevated temperature to real-life service time. Cast cylindrical specimens were exposed to UV radiation, saline water, and various combinations of UV radiation and saline water. These combinations were: a) exposure to saline water followed by UV radiation, b) UV radiation followed by saline water, and c) saline water and then UV radiation followed by saline water. Uniaxial compressive experiments were conducted on both the virgin and exposed specimens at strain rates of $1.7 \times 10^{-3}s^{-1}$ and $2.6 \times 10^{3}s^{-1}$. Under quasi-static loading conditions, the elastic modulus of the polyurea dropped by 73% after 84 days of exposure to saline water at 85 °C. Specimens exposed to UV radiation showed a maximum increase in the elastic modulus of 64% after 20 days of exposure. When tested under dynamic loading conditions, specimens exposed to saline water for 84 days showed a 48% decrease in strain energy while those exposed to UV radiation showed a 45% increase.

1. Introduction

The mechanical behavior of polyurea coatings under quasi-static and dynamic loading conditions after prolonged exposure to saline water (simulating the ocean environment) and ultraviolet (UV) radiation was investigated. Cast cylindrical polyurea specimens were immersed in saline water for a maximum period of 84 days at 85 °C to accelerate the diffusion of water into the elastomer. Additional specimens were exposed to UV radiation at 65 °C in a QUV accelerated tester for a maximum period of 30 days. The remaining specimens were alternatingly exposed to saline water at 65 °C for 14 days and UV radiation at 65 °C for 30 days. The mechanical response of the polyurea before and after exposure to saline water, UV radiation and a combination of saline water and UV radiation was obtained from quasi-static and dynamic uniaxial compression experiments conducted on an Instron 5585 testing machine and a Split Hopkinson Pressure Bar (SHPB) apparatus, respectively.

Faced with an ever-increasing threat on personnel and structures, the marine industry is actively involved in research which can improve durability and survivability of vehicles/structures [1–8]. One of the present solutions for blast/ballistic mitigation is the use of elastomeric coatings on vehicles and structures. Polyurea is one of the elastomers extensively used as a coating material because it has excellent adhesion to most substrates and exhibits exceptional physical properties such as high flexibility, hardness, tear strength, tensile strength, and chemical and water resistance [9]. Early work revealed that adding a polyurea layer on the impact face of an E-glass Vinyl-Ester (EVE) composite plate considerably increases the blast resistance of the plate [1]. Furthermore, using polyurea as an interlayer in a sandwich composite made of EVE facesheets and a monolithically increasing wave impedance foam core material greatly improved the overall blast performance and structural integrity of the sandwich composite, when the polyurea was applied behind the foam core and in front of the back facesheet [2]. Polyurea coatings also have the ability to mitigate the pressure pulses and energy resulting from hydrostatically or explosive initiated underwater implosions, thus reducing the damage on the structure and other neighboring structures [3–5]. The effectiveness of polyurea coatings in mitigating underwater shock is dependent on the material coated, the thickness of the coating, and the location of the coating on the structure itself. For

* Corresponding author.
E-mail address: Shuklaa@uri.edu (A. Shukla).

https://doi.org/10.1016/j.polymertesting.2020.106450
Received 5 December 2019; Received in revised form 4 February 2020; Accepted 18 February 2020
Available online 19 February 2020

example, Pinto and Shukla [3] showed that thick interior coatings on carbon composite tubes significantly reduce the energy released from an underwater implosion by slowing the collapse process and softening wall contact. On the contrary, thick exterior coatings increase the energy by suppressing the damage on the structure, thereby reducing its energy absorption capacity. The blast mitigation potential of polyurea is attributed to a phenomenon commonly referred to as "shock wave capture and neutralization". In the case of high velocity projectile impact, a thick polyurea coating on the back face of a composite system contributes positively towards the reduction of the residual velocity of the projectile, thus increasing the energy absorption of the plate [10]. The ballistic protection ability of polyurea is imputed to its large strain rate dependence, which has been widely investigated in literature. Uniaxial compressive experiments on polyurea under a wide range of strain rates showed that at low strain rates ($2 \times 10^{-3}s^{-1} - 1s^{-1}$), a very small strain rate dependence is noticed in the mechanical behavior of polyurea. Moving from low to high strain rates, ($\tilde{}10^{3}s^{-1}$), there is a transition from a rubbery to a leathery or glassy behavior [11,12]. This same behavior is observed during tensile characterization of polyurea, where there is a reduction in failure strains, increase in failure stress and increase in yield stress as the strain rate increases from low to high [13–15].

Understanding how the mechanical behavior of polyurea is affected by changes in different environmental conditions, such as temperature and pressure, has been widely investigated. Chen et al. [16], through compression experiments on the SHPB, showed that polyurea elastomer exhibited significant temperature sensitivity, with a highly non-linear finite deformation stress – strain behavior. As the temperature was increased, a dynamic softening behavior, and thus a decrease in the flow stress was observed. Increasing the temperatures, with the polyurea under confined pressure, led to less temperature dependence and an approximately linear behavior. The effects of temperature and pressure on the behavior of polyurea have been modeled analytically and numerically [17–20]. Youssef et al. [21,22] examined the effects of UV radiation on the tensile behavior of polyurea plates and revealed that UV radiation increases the stiffness of polyurea plates while rendering them brittle. In addition, prolonged exposure of the plates to UV radiation led to the formation of micro cracks on the surface which caused a drop in the strength of the material. However, the dynamic characterization of polyurea coatings after exposure to aggressive marine environments, principally saline water and UV radiation or an alternating exposure to saline water and UV radiation, has not been investigated.

The present study aims to bridge this gap in knowledge by examining the changes in the mechanical behavior of polyurea coatings after prolonged exposure to aggressive marine environments. Two marine environmental conditions considered in this study were saline water and UV radiation. Three weathering cases were considered; exposure to saline water, exposure to UV radiation, and a combined exposure to saline water and UV radiation. These combinations were: a) exposure to saline water followed by UV radiation, b) UV radiation followed by saline water, and c) saline water and then UV radiation followed by saline water. The exposure to saline water was accelerated in the laboratory by immersing specimens in a saline water bath at an elevated temperature. Water uptake into the cylindrical specimens was measured and finite element analysis was used to model the water uptake into cylindrical specimens. Exposure to UV radiation was accelerated in the laboratory by using a QUV accelerated weathering tester. For each case, compressive stress – strain curves were obtained for different exposure durations, and under quasi - static and dynamic loading conditions.

2. Specimen preparation and experiments

2.1. Material and specimen preparation

Ultra-high strength polyurea (HM-VK) supplied by Specialty Products, Inc. (Lakewood, WA) was used in this study. This polyurea has an average tensile strength of 46.36 MPa (ASTM D638), an elastic modulus of 100 MPa, a maximum elongation of approximately 500%, and a service temperature between −34 °C and 121 °C. Moreover, this polyurea is supplied in two parts, part A and part B, which is mixed in a weight ratio of 1:4, respectively. The gel time is 18 min, which is sufficient for appropriate mixing and molding. The specimens were prepared by mixing the two parts of the polyurea and pouring the mixture into molds of the required specimen geometries. Specimens for the diffusion study were cast as 300 mm long by 25.4 mm wide by 3.2 ± 0.20 mm thick bars and subsequently cut into the required lengths. The specimens for quasi-static and dynamic experiments were cast as cylinders. Specimens for quasi-static experiments were 28.5 mm in diameter and 12.7 mm in length while those for dynamic experiments were 10 mm in diameter and 6 mm in length. The specimen sizes were chosen based on the experimental setups used for quasi-static and dynamic testing. The cast specimens were cured at room temperature for a day and then transferred into an oven at 70 °C for 16 h to ensure that polymerization was completed. The ends of the cylindrical specimens were machined on a lathe and polished to ensure flush contact with the platens during quasi-static and dynamic experiments. All specimens were placed in a desiccator for 24 h prior to exposure to saline water and UV radiation to remove any remaining moisture.

2.2. Saline water exposure

A saline water weathering facility was employed to accelerate the exposure of polyurea specimens to saline water. This facility is composed of a propylene rectangular submerged tank and a rectangular water bath as shown in Fig. 1. The submerged tank contains the specimens exposed to saline water (3.5% NaCl in deionized water). This tank is submerged in the water bath filled with deionized water, which is heated by two immersion heaters and maintained at a constant elevated temperature to accelerate the exposure. The chosen temperature was ensured to fall within the service temperature of polyurea. For specimens exposed exclusively to saline water, the temperature was 85 °C which results in a high acceleration factor. Specimens were exposed at this temperature for a maximum of 84 days. This was a sufficiently long period to simulate years of real-time exposure in the service environment. For combined exposure, the temperature in the saline water bath was reduced to 65 °C and the exposure duration was 14 days. This was because the goal in this set of experiments was for the specimens to reach full saturation. More so, higher temperatures reduce the life span of the heaters. The immersion heaters used were Polyscience LX Immersion Circulators (Cole Parmer, Vernon Hills, IL) with a maximum temperature capacity of 98 °C and a temperature stability of ±0.07 °C. Each heater had a circulating pump that ensured uniform temperature throughout a maximum of 20 L of fluid. Small hollow polypropylene float balls were used to reduce the rate of water evaporation. Water was

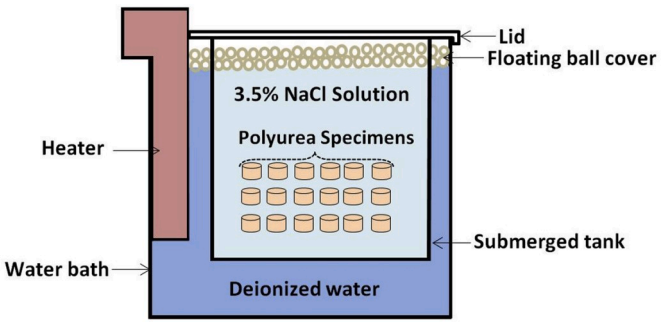

Fig. 1. Schematic of the saline water weathering facility used to expose polyurea specimens to saline water at elevated temperatures. The high temperatures accelerate the aging of the polyurea specimens.

regularly added to the submerged tank to ensure that the salt concentration remained constant. Similarly, water was added to the outside tank to ensure that the water level remained within the range specified for the safe functioning of the heaters.

2.3. UV radiation exposure

The effect of UV radiation on polyurea coatings was investigated by exposing the polyurea specimens to UV radiation in a QUV Accelerated Weathering Tester, by Q-Lab Corporation (Westlake, OH). This facility is designed to simulate outdoor weathering, by exposing materials to UV light at controlled, elevated temperatures. The QUV tester is composed of a base, a central compartment, and a control system as shown in Fig. 2. The central compartment is equipped with eight UVA-340 lamps, which simulate sunlight in the wavelength region from 365 nm down to the solar cutoff of 295 nm. The temperature of the chamber was maintained constant at 65 °C during the exposure of polyurea to UV radiation. This test followed ASTM standard D4329-99 [23]. Polyurea samples were exposed to UV radiation for 10, 20, and 30 days. The side of the specimen facing the UV lamps was changed after half of the exposure time to ensure that both sides of each specimen were exposed to UV radiation for the same duration.

2.4. Determination of the acceleration factor

Prior to exposing the cylindrical specimens to saline water, a diffusion study to determine the acceleration factor (*AF*) was carried out. This acceleration factor is the constant of proportionality relating the time spent in accelerated weathering, $t_{accelerated}$, to its corresponding simulated time in the real-life service environment, t_{actual}, as seen in Equation (1).

$$AF = \frac{t_{accelerated}}{t_{actual}} \tag{1}$$

The approach that was employed to determine the acceleration factor for diffusion in polyurea at an elevated temperature was based on calculating the activation energies involved in the process of diffusion at the operational temperature and at the elevated temperature [24]. This was achieved by immersing polyurea coupons, 76.2 mm long by 25.4 mm wide by 3.2 ± 0.20 mm thick, in the saline water bath at different temperatures and periodically measuring their masses to track the change in mass due to water uptake as per ASTM standard D570 – 98 [25]. The behavior of the material was seen to be Fickian and thus water uptake by the polyurea coupons would be modeled using Fick's second law of diffusion for 1-D, as seen in Equation (2).

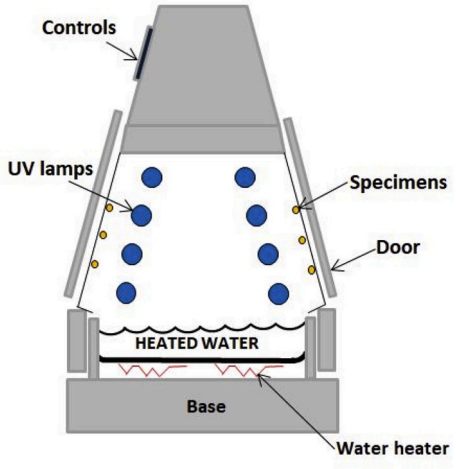

Fig. 2. Schematic of the QUV Accelerated Weathering Tester used to expose polyurea specimens to UV radiation at 65 °C for 30 days.

$$\frac{dC}{dt} = D\frac{d^2C}{dx^2} \tag{2}$$

Where C is the water concentration, D is the diffusion coefficient of water into polyurea, t is the time, and x is the position in the sample. Simplifying assumptions can be made to reduce Equation (2) into Equation (3), which is a form dependent on time and specimen thickness. The assumptions are: the cylinders are initially free of moisture, there is a uniform initial concentration distribution, diffusion occurs at a constant temperature, there is a constant fluid pressure, and the diffusion coefficient is constant [26].

$$\frac{M_t}{M_\infty} = 1 - \frac{8}{\pi^2}\sum_{n=0}^{\infty}\frac{1}{(2n+1)^2}e^{\left[\frac{-D(2n+1)^2\pi^2 t}{4l^2}\right]} \tag{3}$$

Where M_t is the total diffusion substance absorbed by the plate at time t, M_∞ is the quantity of diffusion substance gained after an infinite time (saturation), D is the diffusion coefficient and l is the thickness of the coupon.

The diffusion coefficient can then be calculated from Equation (3) for the five different temperatures (25 °C, 40 °C, 55 °C, 70 °C and 85 °C) using two methods, the method of Aminabhavi et al. [27] and Crank's method [26]. The first method considers that for weight changes below 60% of equilibrium value, Equation (3) can be approximated to Equation (4).

$$\frac{M_t}{M_\infty} = \frac{4}{l}\left(\frac{D}{\pi}\right)^{1/2} t^{1/2} \tag{4}$$

Using Equation (4), the diffusion coefficient for the five different temperatures can be calculated by determining the slope of the linear portion of a plot of normalized mass change against the square root of time. The second method (Crank's method) expresses diffusion in terms of the time at which half of the equilibrium diffusing substance has penetrated the coupon, $\frac{M_t}{M_\infty} = 0.5$, designated as $t_{1/2}$. The diffusion coefficient can then be calculated using Equation (5).

$$D = \frac{0.049l^2}{t_{1/2}} \tag{5}$$

The temperature dependence of the diffusion coefficient was modeled using Arrhenius' equation, which governs the rate of reaction as a function of temperature given by Equation (6a) [28].

$$D = D_0 e^{-\frac{E_a}{RT}} \tag{6a}$$

Where D is the diffusion coefficient, D_0 is the pre-exponential factor, E_a is the activation energy, R is the ideal gas constant, and T is the absolute temperature of the diffusing substance. In order to ease the determination of E_a, Equation (6a) was simplified to obtain the equation of a straight line (Equation (6b)).

$$ln(D) = ln(D_0) - \frac{E_a}{RT} \tag{6b}$$

Once the activation energy was obtained, Equation (7) was used to calculate the acceleration factor, AF.

$$AF = \frac{D_a}{D_w} = \frac{D_0 e^{\frac{E_a}{RT_a}}}{D_0 e^{\frac{E_a}{RT_w}}} = e^{\frac{E_a}{R}\left(\frac{1}{T_w} - \frac{1}{T_a}\right)} \tag{7}$$

Where D_a is the diffusion coefficient for accelerated laboratory testing at a temperature T_a, and D_w is the diffusion coefficient at the normal working or service temperature, T_w in Kelvin.

2.5. Experimental set-up and procedure

The quasi-static stress – strain response of the polyurea coatings was experimentally obtained using a standard screw driven mechanical testing machine, Instron 5585. The dynamic behavior was obtained using a modified SHPB apparatus as shown in Fig. 3.

The incident and transmission bars were made from 6061-T6 Aluminum. The incident bar had a diameter of 19.1 mm and a length of 1.83 m. A 1.22 m long hollow transmitter bar with a 19.1 mm outer diameter and 16.5 mm inner diameter was used to decrease the cross-sectional area of the bar and consequently increase the strains on the transmitted bar. Thus, the hollow transmitter bar worked as a linear elastic stress/strain amplifier. This hollow transmitter bar had tightly fitted aluminum 6061-T6 endcaps. A pair of resistive strain gages (C2A-13-250LW-350) from Vishay Measurements Group was attached in the middle of each bar. Gages on each bar were bonded opposite to each other to cancel the effect of any bending that could occur during the experiment. These strain gages were employed to measure the incident, reflected and transmitted pulses. A pulse shaper was used at the impact end of the incident bar, to facilitate dynamic stress equilibrium, minimize the radial inertia in the specimens and obtain a nearly constant strain rate during deformation. Pulse shapers were created by rolling clay on a sheet of paper to a thickness of 1.2 mm and punching out 6.0 mm diameter disc from the paper-clay composite material. A thin layer of molybdenum disulfide lubricant was applied between the specimen surface and the contacting bar end faces to minimize the friction effects. The stress, strain rate, and strain after the specimen deformed under dynamic stress equilibrium were calculated using Equations (8)–(10), respectively [29].

$$\sigma = \frac{A_t}{A_i} E_0 \varepsilon_t(t) \tag{8}$$

$$\dot{\varepsilon} = -\frac{C_0}{L_s} \varepsilon_r(t) \tag{9}$$

$$\varepsilon = \frac{C_0}{L_s}\left(1 - \frac{A_t}{A_i}\right)\int_0^t \varepsilon_i(t)dt - \frac{C_0}{L_s}\left(1 + \frac{A_t}{A_i}\right)\int_0^t \varepsilon_r(t)dt \tag{10}$$

Where C_0 is the wave velocity in the bar material, L_s is the original length of the specimen, A_i and A_t are the cross-sectional areas of the incident and transmission bars, respectively. $\varepsilon_i(t)$, $\varepsilon_r(t)$, and $\varepsilon_t(t)$ are the incident, reflected and transmitted strain histories, respectively. These equations are different from those of the conventional SHPB due to the difference in the cross-sectional areas of the incident and the transmitter bars. The true stress and strain were calculated using Equations (11) and (12), respectively.

$$\sigma_s = \sigma(1 - \varepsilon) \tag{11}$$

$$\varepsilon_s = -ln(1 - \varepsilon) \tag{12}$$

The incident, reflected, and transmitted pulses from a typical high strain rate experiment on a non-weathered specimen are shown in Fig. 4a. The initial strain acceleration is lowered and most of the high frequency oscillations are eliminated by using the pulse shaper. A typical dynamic stress equilibrium plot is shown in Fig. 4b. This illustrates the force on the front and back face of the specimen. Dynamic stress equilibrium is verified between 20 μs and 150 μs. Lastly, Fig. 4c shows the strain history with an almost constant strain rate between 50 μs and 150 μs.

3. Results and discussion

3.1. Water diffusion

3.1.1. Acceleration factor

The mass change during immersion of the polyurea coupons normalized by maximum mass change, for different temperatures, is plotted as a function of the square root of time as seen in Fig. 5. This plot shows that at the onset of immersion, water uptake is directly proportional to the square root of time, and as the immersion time increases, the water uptake reduces, and a plateau is reached at saturation. This behavior is a typical Fickian behavior and the water uptake by the polyurea coupons was modeled using Fick's second law of diffusion for 1-D, as seen in Equation (2).

The diffusion coefficient was calculated for the five different temperatures using the method by Aminabhavi et al. [27] and Crank's method [26]. With the calculated diffusion coefficients, the respective logarithmic values were plotted against the inverse of the corresponding absolute temperature, shown in Fig. 6. The two methods used for the calculation of the diffusion coefficients gave similar results. In addition, from Fig. 5, it is seen that water diffusion kinetics is dependent on the temperature. Even though the initial water uptake was constant for all temperatures, the coupons immersed in saline water at higher temperatures reached saturation faster than those at lower temperatures. The temperature dependence of the diffusion coefficient was modeled using Arrhenius' equation, which governs the rate of reaction as a function of

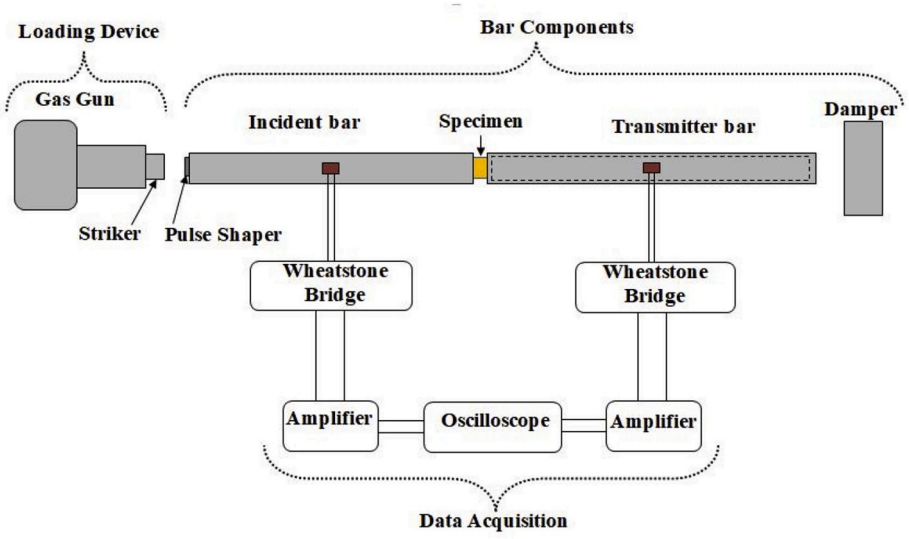

Fig. 3. Schematic of the modified Split Hopkinson pressure bar with a hollow transmitter bar, designed for soft materials characterization.

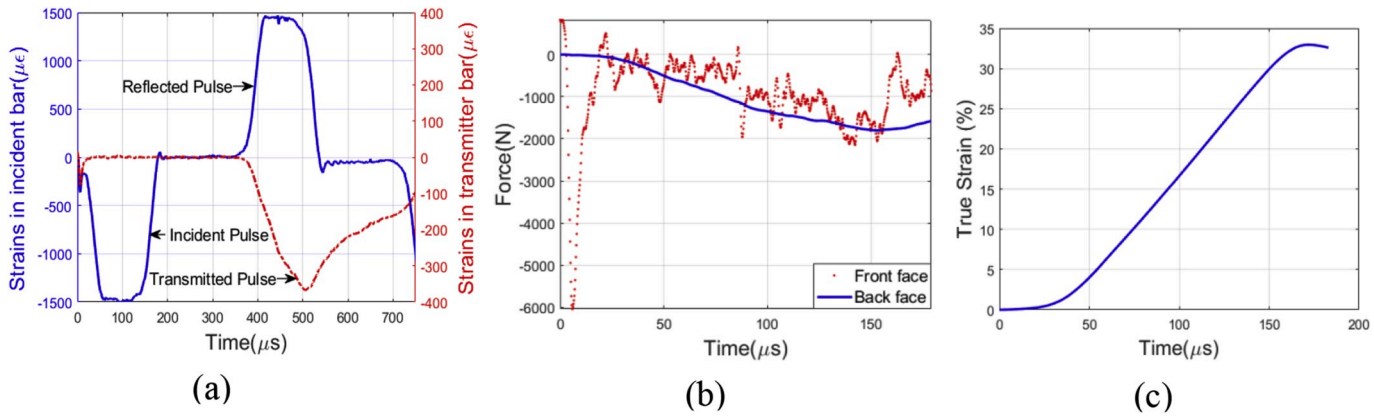

Figure 4. (a) – Incident, reflected and transmitted pulses from the SHPB, (b) – Dynamic stress equilibrium in polyurea specimen, (c) – Strain history for unexposed polyurea specimens.

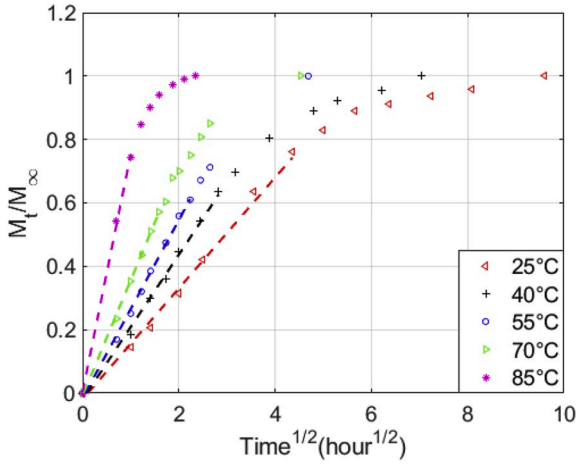

Fig. 5. Average normalized mass change during immersion of polyurea in saline water for five different temperatures.

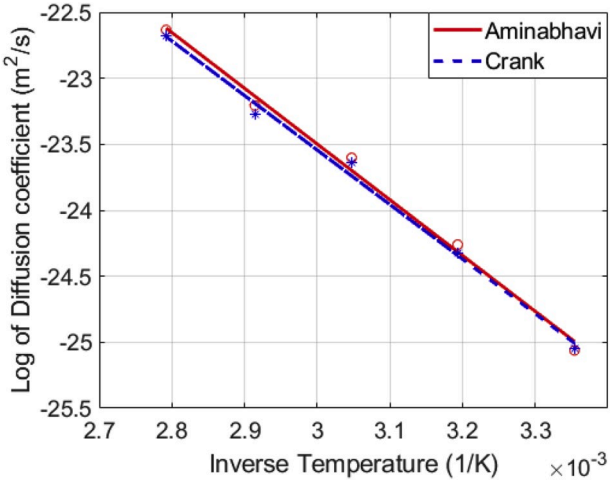

Fig. 6. Determination of the activation energy for water diffusion into polyurea coupons.

temperature and the activation energy.

Once the activation energy was obtained from Equation (6b), Equation (7) was used to calculate the acceleration factor, AF. The acceleration factor was computed to be 15.86 for an average ocean (service) temperature of 17 °C and an elevated (accelerated weathering) temperature of 85 °C. Thus, an accelerated weathering period of 84 days (maximum exposure time for polyurea specimens) is equivalent to approximately 4 years of real-life exposure to sea water. Also, when using 65 °C (which was the temperature used for combined exposure) as the elevated temperature, the acceleration factor was determined to be 7.90. Thus, 14 days of accelerated weathering in saline water at 65 °C give about 4 months of real-life weathering.

3.1.2. *Mass change in the polyurea during exposure to saline water*

The percent mass change as a function of the square root of immersion time, for the cylindrical specimens, is shown in Fig. 7. This graph can be divided into three regions: a positive slope region, a plateau or zero slope region, and a negative slope region. The positive slope region starts with an initial rapid, linear increasing part, followed by a slow nonlinear increase. This region shows a rapid initial water uptake which can be attributed to a high diffusion gradient at the beginning of the diffusion process. The rate of water uptake decreases with a decrease in the diffusion gradient between the saline water and the specimen.

For specimens used in quasi-static and dynamic experiments, this region lasts for 78 h and 14 h, respectively. The plateau region corresponds to saturation of the polyurea specimens. The percentage mass change at saturation was about 2.5% for both specimens. The negative slope region indicates a decrease in the mass of the elastomeric coating, which can be attributed to the leaching of degradation products coming

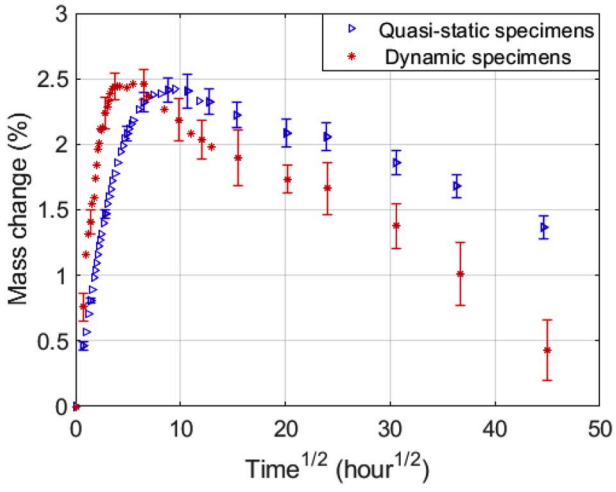

Fig. 7. Percent mass change in polyurea specimens during exposure to saline water for 84 days at 85 °C.

from the hydrolysis of polyurea [30]. The specimens used for dynamic experiments showed a faster percent mass change than the specimens for the quasi-static experiments. This rapid change can be attributed to the high surface to volume ratio of the specimens used in dynamic experiments, which was 2.6 times the surface to volume ratio of the specimens used in quasi-static experiments.

3.1.3. Numerical modeling of water uptake in polyurea

The process of water uptake in cylindrical specimens was modeled numerically to obtain the time taken for the cylindrical polyurea specimens to reach saturation, when immersed in saline water at different elevated temperatures. This model employed Fick's second law of diffusion in cylindrical coordinates, shown in Equation (13).

$$\frac{\partial C}{\partial t}=\frac{1}{r}\frac{\partial}{\partial r}\left(Dr\frac{\partial C}{\partial r}\right)+\frac{1}{r^2}\frac{\partial}{\partial \theta}\left(D\frac{\partial C}{\partial \theta}\right)+\frac{\partial}{\partial x}\left(D\frac{\partial C}{\partial x}\right) \tag{13}$$

Considering axisymmetry in the cylindrical specimens, Equation (13) reduces to Equation (14).

$$\frac{\partial C}{\partial t}=\frac{1}{r}\frac{\partial}{\partial r}\left(Dr\frac{\partial C}{\partial r}\right)+\frac{\partial}{\partial x}\left(D\frac{\partial C}{\partial x}\right) \tag{14}$$

This differential equation was solved numerically, for the specimens used in dynamic and quasi-static characterization. The diffusion coefficient obtained in the diffusion study for the temperature of 85 °C was employed in the numerical calculations. A triangular element mesh was used in the finite element analysis and random nodes were chosen along the radius of the specimen. The variation in concentration on the center plane along the radius was determined for a period of 160 h and 40 h for the specimens used in quasi-static and dynamic experiments, respectively. These results are shown in Fig. 8a and b respectively. From the plots, during the first few minutes of immersion, water concentration increases rapidly for nodes close to the surface of the specimen. At this time, nodes close to the center remain at almost zero concentration. As the nodes close to the surface approach saturation, the water concentration of nodes close to the center rapidly increases. The experimental mass change for both specimen geometries was also plotted on the right axes of Fig. 8a and b. From the figures, the experimentally obtained mass change shows an excellent correlation with numerical results.

3.2. Mass change in the polyurea during exposure to UV radiation

Fig. 9 shows the percent mass change observed when polyurea specimens were exposed to UV radiation for 720 h (30 days). Both specimens showed an initial rapid decrease in mass, which is mostly due to the loss of moisture that was present in the specimens prior to exposure. Besides, scission of bonds occurred between carbon and hydrogen atoms in the polymer chains, leading to the formation of free radicals and consequently a reduction in the molecular weight of the initial polymer chain. This bond scission also created room for cross-linking between polymer chains, eventually leading to the formation of longer polymer chains. The cross-linking process was initiated physically by the UV radiation. The decrease in mass was faster in the specimens for quasi-static experiments. The region of the rapid percent decrease in mass was closely followed by a slow mass loss. After 400 h, the specimens for dynamic experiments showed almost no further change whereas the specimens for the quasi-static experiments showed a small decrease in the mass. At the end of 30 days, the specimens for quasi-static and dynamic experiments showed a mass loss of 1.8% and 2.0%, respectively.

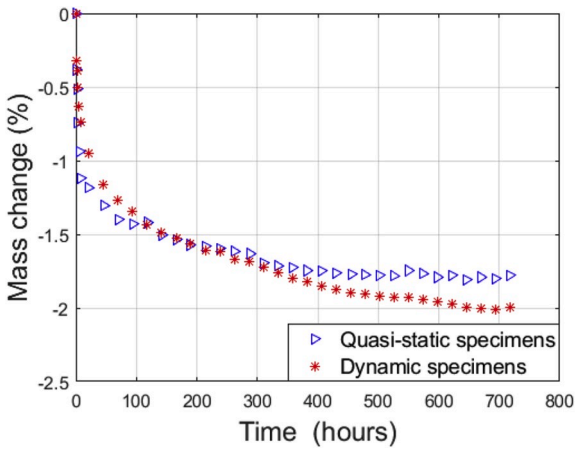

Fig. 9. Percent mass change in polyurea specimens during exposure to UV radiation.

3.3. Quasi-static and dynamic behavior of polyurea after exposure to saline water and UV radiation

3.3.1. Exposure to saline water

The resultant compressive true stress vs true strain curves for polyurea coatings exposed to saline water for different durations, under quasi-static and dynamic loading conditions are presented in Fig. 10a and b, respectively. Each curve represents the average of five repeated experiments conducted under identical loading conditions. Error bars were plotted on each mean stress – strain curve to show data dispersion. Quasi-static and dynamic experiments were conducted at a strain rate of $1.7 \times 10^{-3}s^{-1}$, and $2.6 \times 10^{3}s^{-1}$, respectively. All stress – strain curves exhibit an initial linear region, which increasingly becomes non-linear as the strain increases. For the specimens subjected to quasi-static

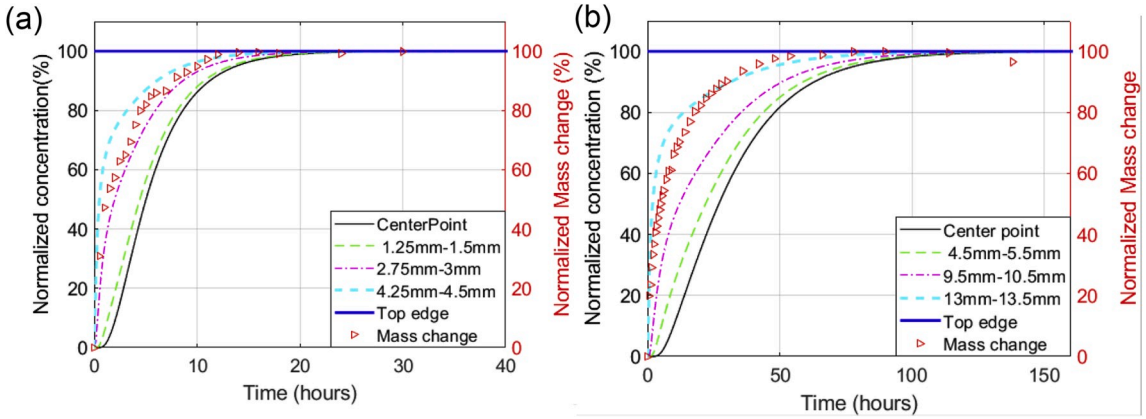

Fig. 8. Variation of water concentration along the radius of polyurea cylindrical specimens (left axis), compared to mass change from experiments (right axes)(a) – specimen for quasi-static experiments (b) – specimen for dynamic experiments.

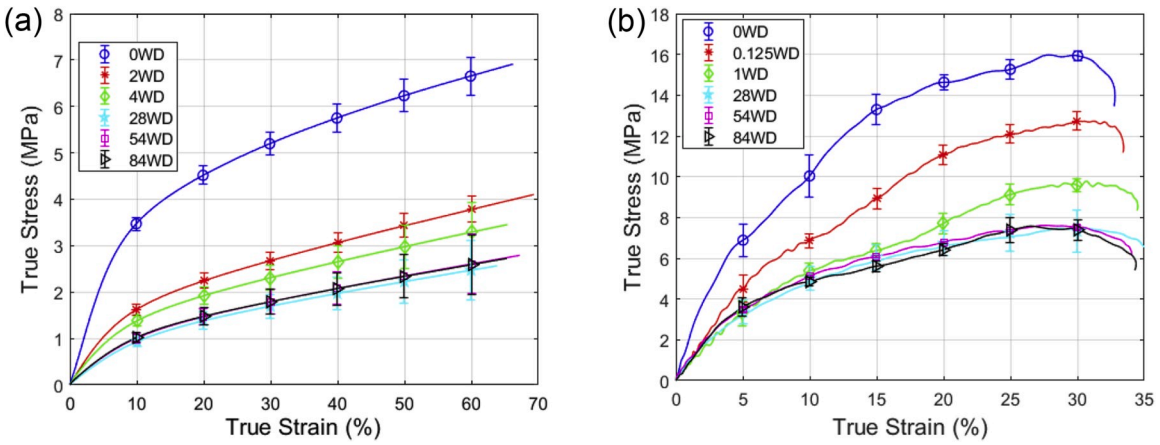

Fig. 10. Uniaxial compressive stress – strain behavior of polyurea exposed to saline water for different time durations (a) – Quasi-static behavior (b) – Dynamic behavior.

loading, statistical analysis using student t-test with a 95% level of confidence showed that there was a significant decrease in the elastic modulus by 53% within the first two days (2WD) of exposure. The modulus of elasticity continued to drop gradually as seen in case of four days (4WD) until saturation where it stabilized. After 84 days of exposure, a total decrease in the modulus of elasticity of about 73% was recorded. The loss in the elastic modulus can be attributed to hydrolysis of the polymer which led to scission of polymer chains, thus weakening the polyurea coating. The strain energy, which is seen as mechanical energy stored in the polyurea and which is the property that determines the energy absorption potential of polyurea, was calculated for different durations of exposure at 25% strains. The results are presented on Table 1 and show that exposure of polyurea to saline water led to a rapid decrease in the strain energy from 0.85 ± 0.02 MJ/m^3 for virgin specimens to 0.41 ± 0.01 MJ/m^3 after two days of exposure, and then a slow decrease to 0.26 ± 0.03 MJ/m^3 for specimens exposed for 84 days. For the specimens that were subjected to dynamic loading conditions, a similar trend in the behavior of polyurea was observed. The dynamic modulus of elasticity could not be calculated from the stress – strain plots since there was no force equilibrium in the specimens during the first 20μs of experimentation. Nevertheless, the strain energy calculations at 25% strain indicated that there was a drop in the strain energy from 2.67 ± 0.12 MJ/m^3 for virgin specimens to 1.91 ± 0.07 MJ/m^3 after 0.125 day of exposure (0.125WD). The strain energy continued to decrease to 1.40 ± 0.1207 MJ/m^3 after 1 day of exposure (1WD) and to 1.27 ± 0.09 MJ/m^3 for specimens exposed for 84 days. Note that lower exposure times were considered for the specimens used in the dynamic experiments because the diffusion in these specimens was faster as a result of a higher surface to volume ratio. Although the behavior of polyurea coatings subjected to dynamic loading conditions showed a similar trend in the degradation of the material, strain rate dependence of the material before and after exposure to saline water was evident. For virgin specimens, at 25% true strains, the true stress was 4.88 ± 0.19 MPa for quasi-static response and 15.29 ± 0.32 MPa for the dynamic response, giving about 213% increase in the true stress. This increase is observed because at high strain rates, polyurea stiffens, thus behaves as leather instead of a rubbery material. Similarly, at 25% strains, the strain energy at high strain rate was 214% higher than the strain energy at low strain rate. The change in true stress and strain energy for specimens exposed to saline water was more drastic. The true stress after 84 days of exposure for quasi-static and dynamic specimens was 1.64 ± 0.22 MPa and 7.41 ± 0.48 MPa, respectively, giving 350% increase in the true stress. The strain energy at high strain rate was 390% higher than the strain energy at low strain rate.

It should be noted that after saturation, there was a statistically insignificant difference in the stress – strain behavior of the polyurea. More specifically, for 28, 56 and 84 days of exposure, the stresses for the same strain levels were approximately the same, even though from Fig. 7, there was a continuous reduction in the mass of the specimens during that exposure period. This shows that water uptake is the main process governing material degradation.

Table 1
Strain energy for polyurea with exposure to saline water.

Quasi-static Experiments		Dynamic Experiments	
Duration of Exposure (Days)	Strain energy at 25% strain (MJ/m^3)	Duration of Exposure (Days)	Strain energy at 25% strain (MJ/m^3)
0	0.85 ± 0.02	0	2.67 ± 0.12
2	0.41 ± 0.01	0.125	1.91 ± 0.07
4	0.35 ± 0.02	1	1.40 ± 0.12
28	0.24 ± 0.05	28	1.26 ± 0.16
56	0.26 ± 0.06	56	1.28 ± 0.01
84	0.26 ± 0.03	84	1.27 ± 0.09

3.3.2. *Exposure to UV radiation*

Fig. 11a and b show the resultant uniaxial compressive stress – strain curves for polyurea specimens exposed to UV radiation at 65 °C for 10, 20, and 30 days, under quasi-static and dynamic loading conditions, respectively. The trend in the stress – strain behavior is same as that for exposure to saline water except that strain hardening is evident after 40% strain, in the polyurea coatings exposed to UV radiation. All stress – strain curves display an increase in the elastic modulus and strain energy for the polyurea coatings after exposure to UV radiation. Particularly, in the case of quasi-static loading conditions ($\dot{\varepsilon} = 1.7 \times 10^{-3} s^{-1}$), there was a statistically significant increase in the modulus of elasticity by 57%, 64% and 56% after 10, 20 and 30 days of exposure, respectively. This same trend was seen in the true stress at 25% strains which increased from 5.21 ± 0.19 MPa to 6.54 ± 0.05 MPa after the first 10 days of exposure. The true stress further increased to 6.77 ± 0.09 MPa after 20 days and then a slight drop in the true stress to a value of 6.50 ± 0.50 MPa was noticed for specimens exposed to UV radiation for 30 days. The increase in the modulus of elasticity and true stress for the first 20 days of exposure is attributed to photo-degradation and photo-oxidation, which involve cross-linking in polymer chains initiated by the UV radiation [22]. Nevertheless, the increase in stiffness rendered the coatings brittle, and longer periods of exposure led to the creation of micro cracks on the surface which weakened the polyurea coating and led to a drop in the elastic modulus and true stress as seen after 30 days of exposure. The strain energy at 25% strains showed an increase by 33%, 35% and 29% after 10, 20 and 30 days of exposure to UV radiation, respectively, as seen in Table 2. These results can be correlated to the

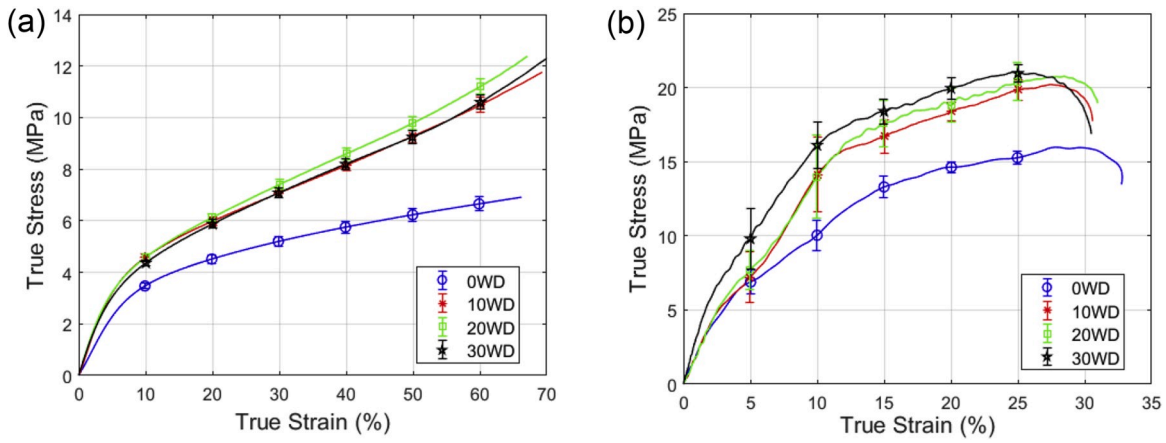

Fig. 11. Uniaxial compressive stress – strain behavior of polyurea exposed to UV radiation for different time durations (a) – Quasi-static behavior (b) – Dynamic behavior.

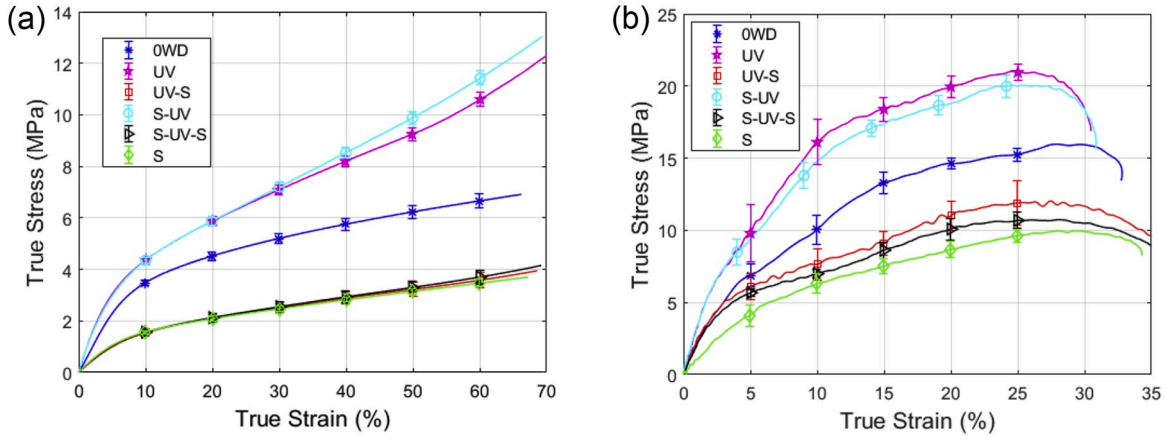

Fig. 12. Uniaxial compressive stress – strain behavior of polyurea when alternatingly exposed to saline water and UV radiation (a) - Quasi-static behavior (b) - Dynamic behavior.

mass change seen in Fig. 9, which show a very small mass change between 10 days (240 h) and 20 days (480 h). Beyond the 20 days, the mass was approximately constant indicating no photo-oxidation within this period and thus no stiffening of the coatings.

In the case of dynamic loading ($\dot{\varepsilon} = 2.6 \times 10^3 s^{-1}$), considering 25% strains, there was an increase in the true stress from 15.29 ± 0.32 MPa to 20.05 ± 0.67 MPa after 10 days of exposure. The true stress kept increasing slowly to 20.67 ± 1.48 MPa and then to 21.114 ± 0.45 MPa as exposure time increases to 20 and 30 days, respectively. This same trend was seen in the strain energy where the energy increased by 29%, 34% and 45% for 10, 20 and 30 days of exposure, respectively. The continuous change in true stress and strain energy of polyurea coatings subjected to dynamic loading can be correlated to the continuous loss in the mass of the specimens for dynamic experiments throughout the exposure duration as shown in Fig. 9.

Both weathered and non-weathered polyurea coatings showed higher true stresses at a higher strain rate. For the specimens exposed to UV radiation for 30 days, the true stress at 25% strains increased from 6.50 ± 0.12 MPa to 21.11 ± 0.50 MPa. In addition, the strain energy increased by 254% for specimens exposed to UV radiation for 30 days, indicating that polyurea coatings exposed to UV radiation are strain-rate sensitive.

Table 2
Strain energy for polyurea with exposure to UV radiation.

Quasi-static Experiments		Dynamic Experiments
Duration of Exposure (Days)	Strain energy at 25% strain (MJ/m^3)	Strain energy at 25% strain (MJ/m^3)
0	0.85 ± 0.02	2.67 ± 0.12
10	1.13 ± 0.01	3.44 ± 0.12
20	1.15 ± 0.01	3.54 ± 0.52
30	1.10 ± 0.02	3.88 ± 0.26

3.3.3. Combined exposure of polyurea to saline water and UV radiation

Fig. 12a and b show the uniaxial true stress vs true strain response of polyurea exposed alternatingly to saline water and UV radiation and tested under quasi-static and dynamic loading conditions, respectively. Three combinations were considered in this study: pre-exposing polyurea to UV radiation before immersion in saline water, pre-exposing polyurea to saline water before exposing to UV radiation, and pre-exposing polyurea to saline water, exposing the polyurea to UV radiation and re-exposing it to saline water. The stress – strain behavior for virgin polyurea specimens (0WD), polyurea specimens exposed exclusively to UV radiation, and polyurea specimens exposed solely to saline water are plotted together, to facilitate comparison. Comparison was done using true stress and strain energy calculated at 25% strains for all cases.

In the case of quasi-static loading ($\dot{\varepsilon} = 1.7 \times 10^{-3} s^{-1}$), the stress – strain response of polyurea specimens pre-exposed to UV radiation before immersion in saline water does not show any noticeable difference when compared to the behavior of polyurea specimens immersed exclusively in saline water for same duration. The mean true stress and

strain energy at 25% strains in both cases are 3.3 MPa and 0.39 MJ/m^3, respectively. Similar results are obtained when polyurea is pre-immersed in saline water, exposed to UV radiation and re-exposed to saline water. For the polyurea specimens exposed to saline water before UV radiation, the true stress and strain energy obtained are 6.53 ± 0.28 MPa and 1.10 ± 0.03 MJ/m^3, respectively. This is also not statistically different from the true stress and strain energy obtained in the case of polyurea specimens exposed exclusively to UV radiation as seen in Table 3.

The response of polyurea coatings under dynamic loading conditions ($\dot{\varepsilon} = 2.6 \times 10^3 s^{-1}$) showed differences as revealed in Fig. 12b. The true stress at 25% strains for polyurea specimens pre-exposed to UV radiation before immersion in saline water was 11.87 ± 1.31 MPa. This is 22% higher than the true stress for polyurea specimens exposed solely to saline water. The computed strain energy for polyurea specimens pre-exposed to UV radiation before immersion in saline water was also 26% higher than the strain energy for polyurea specimens exposed exclusively to saline water. This difference in true stress and strain energy in the case of the specimens for dynamic experiments can be imputed to the small thickness of the specimens. The specimen thickness permits the penetration of UV radiation through the entire thickness, thus more cross-linking of polymer chains. Therefore, immersing these specimens in saline water will need more time for the polymer chains to be broken in the process of hydrolysis. The true stress and strain energy computed for specimens pre-exposed to saline water before exposure to UV radiation were respectively 20.18 ± 0.89Mpa and 3.65 ± 0.16 MJ/m^3. These values are 4% and 6% lower than the true stress and strain energy for specimens exposed solely to UV radiation. It is seen that pre-exposing the coatings to saline water before UV radiation leads to a much longer time for moisture loss and cross-linking in the QUV. Lastly, specimens exposed to saline water, UV radiation and then saline water, showed respectively 11% and 15% higher true stress and strain energy values when compared to specimens exposed solely to saline water, and respectively 9.4% and 8.9% lower true stress and strain energy values when compared to specimens pre-exposed to UV radiation before immersion in saline water. This is because when the specimens were immersed in saline water and then exposed to UV radiation, their strain energy was less than that of specimens exposed exclusively to UV radiation as earlier explained. When these specimens, which had not had enough time to reach maximum cross-linking initiated by UV radiation, were immersed in saline water, bond scission due to hydrolysis took place. This led to a drop in the strain energy of the polyurea specimens to a value higher than that of specimens exposed solely to saline water, and lower than that of specimens pre-exposed to UV radiation before immersion in saline water. From these results, it can be concluded that more cross-linking occurs in thinner coatings as the entire thickness is affected by UV radiation. For very thick coatings, the effect of UV radiation is felt more on the surface and the central region of the specimen is almost unaffected.

4. Conclusions

This study experimentally investigated the mechanical behavior of polyurea coatings after prolonged exposure to aggressive marine environments. Uniaxial compressive experiments were conducted on polyurea coatings after exposure to two different marine conditions, saline water and UV radiation. The behavior of the coatings under alternating weathering conditions was also investigated. The response of the polyurea coatings was determined under quasi-static and dynamic loading conditions. The completion of this study led to following conclusions:

(1) Using the acceleration factor obtained from the diffusion study, exposing polyurea specimens to saline water for 84 days at 85 °C is equivalent to 4 years of real-life exposure to sea water.
(2) Polyurea coatings exposed to saline water showed a maximum percent increase in mass of 2.5% and a decrease in elastic modulus of approximately 73% after 84 days of exposure at a temperature of 85 °C. The drastic drop in the elastic modulus of the coatings was attributed to scission of polymer chains due to hydrolysis. After exposure to saline water for 84 days, the energy absorption capability of the polyurea coatings decreased by 69% and 48% for specimens used for quasi-static and dynamic experiments, respectively.
(3) Exposure of polyurea coatings to UV radiation for 30 days at 65 °C led to a maximum mass loss of 1.8% and 2.0% for specimens used in quasi-static and dynamic experiments, respectively. A maximum increase in elastic modulus and strain energy of 64% and 35%, respectively was recorded after exposure to UV radiation for 20 days. This increase in elastic modulus and strain energy was as a result of cross-linking between polymer chains, initiated by UV radiation. Specimens for dynamic experiments showed a maximum increase of 45% in strain energy after 30 days of exposure.
(4) During quasi-static loading, there was no significant difference in the mechanical behavior of specimens pre-exposed to UV radiation before immersion in saline water, compared to polyurea specimens exposed exclusively to saline water, and polyurea specimens exposed to saline water, UV radiation and re-exposed to saline water. Similarly, specimens pre-exposed to saline water before UV radiation did not show any statistically significant difference when compared to specimens exposed solely to UV radiation. On the other hand, specimens used in dynamic experiments which underwent combined weathering showed significant differences in the true stress and strain energy when compared to specimens exposed exclusively to saline water or UV radiation. Specimens pre-exposed to UV radiation before immersion in saline water showed a 26% increase in strain energy, when compared to specimens without pre-exposure. Specimens pre-exposed to saline water before UV radiation showed a 6% decrease in strain energy when compared to specimens exposed exclusively to UV radiation. Also, specimens which were immersed in saline water, exposed to UV radiation and re-immersed in saline water showed a 15% increase in the strain energy, when compared to specimens exposed solely to saline water.
(5) Increasing the strain rate from $1.7 \times 10^{-3} s^{-1}$ to $2.6 \times 10^3 s^{-1}$ led to consistent increase in the true stress and strain energy, in both virgin and weathered polyurea coatings. For virgin polyurea coatings, there was an increase in the true stress and strain energy of 213% and 214%, respectively. Polyurea coatings exposed to saline water showed a 350% and 390% increase in the true stress and strain energy, respectively. For exposure to UV radiation, there was an increase in the true stress and strain energy of 225% and 254%, respectively. This shows that polyurea is strain rate dependent before and after exposure to aggressive marine environments.

Table 3
Strain energy for polyurea with combined exposure to saline water and UV radiation.

Quasi-static Experiments		Dynamic Experiments
Duration of Exposure (Days)	Strain energy at 25% strain (MJ/m^3)	Strain energy at 25% strain (MJ/m^3)
0WD	0.85 ± 0.02	2.67 ± 0.12
UV	1.10 ± 0.02	3.89 ± 0.26
UV-S	0.39 ± 0.01	2.03 ± 0.04
S-UV	1.10 ± 0.03	3.65 ± 0.16
S-UV-S	0.39 ± 0.01	1.85 ± 0.09
S	0.39 ± 0.01	1.61 ± 0.21

Declaration of competing interest

The authors declare that they have no known competing financial interests or personal relationships that could have appeared to influence the work reported in this paper.

CRediT authorship contribution statement

Irine Neba Mforsoh: Conceptualization, Methodology, Investigation, Visualization, Writing - original draft. **James LeBlanc:** Conceptualization, Methodology, Formal analysis, Visualization, Writing - review & editing. **Arun Shukla:** Conceptualization, Methodology, Supervision, Visualization, Writing - review & editing.

Acknowledgment

The authors kindly acknowledge the financial support provided by Dr. Elizabeth Magliula from the Naval Engineering Education Consortium (NEEC) Grant No. N00174-19-1-0005. The authors also acknowledge their colleagues in the Dynamic Photo-Mechanics Laboratory, especially Dr. Prathmesh Naik Parrikar, Taylor Smith and Daynamar Delgado Nieves for their dedicated help in the preparation and execution of experiments.

Appendix A. Supplementary data

Supplementary data to this article can be found online at https://doi.org/10.1016/j.polymertesting.2020.106450.

References

[1] S.A. Tekalur, A. Shukla, K. Shivakumar, Blast resistance of polyurea based layered composite materials, Compos. Struct. 84 (2008) 271–281, https://doi.org/10.1016/j.compstruct.2007.08.008.
[2] N. Gardner, E. Wang, P. Kumar, A. Shukla, Blast mitigation in a sandwich composite using graded core and polyurea interlayer, Exp. Mech. 52 (2012) 119–133, https://doi.org/10.1007/s11340-011-9517-9.
[3] M. Pinto, A. Shukla, Mitigation of pressure pulses from implosion of hollow composite cylinders, J. Compos. Mater. 50 (2016) 3709–3718, https://doi.org/10.1177/0021998315624254.
[4] H. Matos, A. Shukla, Mitigation of implosion energy from aluminum structures, Int. J. Solid Struct. 101 (2016) 566–574, https://doi.org/10.1016/j.ijsolstr.2016.09.030.
[5] E. Gauch, J. Leblanc, A. Shukla, Near field underwater explosion response of polyurea coated composite cylinders, Compos. Struct. 202 (2018) 836–852, https://doi.org/10.1016/j.compstruct.2018.04.048.
[6] C. Shillings, C. Javier, J. Leblanc, C. Tilton, L. Corvese, A. Shukla, Experimental and computational investigation of the blast response of Carbon-Epoxy weathered composite materials, Composites Part B 129 (2017) 107–116, https://doi.org/10.1016/j.compositesb.2017.07.023.
[7] C. Javier, H. Matos, A. Shukla, Hydrostatic and blast initiated implosion of environmentally degraded Carbon-Epoxy composite cylinders, Compos. Struct. 202 (2018) 897–908, https://doi.org/10.1016/j.compstruct.2018.04.055.
[8] H. Matos, C. Javier, J. Leblanc, A. Shukla, Underwater nearfield blast performance of hydrothermally degraded carbon – epoxy composite structures, Multiscale Multidiscip. Model. Exp. Des. 1 (2018) 33–47, https://doi.org/10.1007/s41939-017-0004-6.
[9] N. Iqbal, M. Tripathi, S. Parthasarathy, D. Kumar, P.K. Roy, Polyurea coatings for enhanced blast-mitigation : a review, RSC Adv. 6 (2016) 109706–109717, https://doi.org/10.1039/c6ra23866a.
[10] D. Mohotti, T. Ngo, P. Mendis, S.N. Raman, Polyurea coated composite aluminum plates subjected to high velocity projectile impact, Mater. Des. 52 (2013) 1–16, https://doi.org/10.1016/j.matdes.2013.05.060.
[11] J. Yi, M.C. Boyce, G.F. Lee, E. Balizer, Large deformation rate-dependent stress – strain behavior of polyurea and polyurethanes, Polymer 47 (2006) 319–329, https://doi.org/10.1016/j.polymer.2005.10.107.
[12] J. Shim, D. Mohr, Using split Hopkinson pressure bars to perform large strain compression tests on polyurea at low, intermediate and high strain rates, Int. J. Impact Eng. 36 (2009) 1116–1127, https://doi.org/10.1016/j.ijimpeng.2008.12.010.
[13] C.M. Roland, J.N. Twigg, Y. Vu, P.H. Mott, High strain rate mechanical behavior of polyurea, Polymer 48 (2007) 574–578, https://doi.org/10.1016/j.polymer.2006.11.051.
[14] S.N. Raman, T. Ngo, J. Lu, P. Mendis, Experimental investigation on the tensile behavior of polyurea at high strain rates, Mater. Des. 50 (2013) 124–129, https://doi.org/10.1016/j.matdes.2013.02.063.
[15] V.S. Joshi, C. Milby, A. You, M.A.Y. Be, High strain rate behavior of polyurea compositions, in: AIP Conference Proceedings, vol. 1426, 2012, pp. 1–5, https://doi.org/10.1063/1.3686246, 167.
[16] Y. Chen, B. Cheng, Y. Xiao, Experimental investigation on dynamic compressive behavior of polyurea over a range of temperatures, Int. J. Sci. Technol. 5 (2016) 457–461.
[17] A.V. Amirkhizi, J. Isaacs, J. McGee, S. Nemat-Nasser, An experimentally-based viscoelastic constitutive model for polyurea, including pressure and temperature effects, Phil. Mag. 86 (2006) 5847–5866, https://doi.org/10.1080/14786430600833198.
[18] C. Gamonpilas, R. McCuiston, A non-linear viscoelastic material constitutive model for polyurea, Polymer 53 (2012) 3655–3658, https://doi.org/10.1016/j.polymer.2012.06.030.
[19] H. Guo, W. Guo, A.V. Amirkhizi, R. Zou, K. Yuan, Experimental investigation and modeling of mechanical behaviors of polyurea over wide ranges of strain rates and temperatures, Polym. Test. 53 (2016) 234–244, https://doi.org/10.1016/j.polymertesting.2016.06.004.
[20] C. Li, J. Lua, A hyper-viscoelastic constitutive model for polyurea, Mater. Lett. 63 (2009) 877–880, https://doi.org/10.1016/j.matlet.2009.01.055.
[21] G. Youssef, I. Whitten, Dynamic properties of ultraviolet-exposed polyurea, Mech. Time-Dependent Mater. 21 (2017) 351–363, https://doi.org/10.1007/s11043-016-9333-9.
[22] G. Youssef, J. Brinson, I. Whitten, The effect of ultraviolet radiation on the hyperelastic behavior of polyurea, J. Polym. Environ. 26 (2018) 183–190, https://doi.org/10.1007/s10924-016-0933-x.
[23] ASTM D 4329-99, Standard Practice for Fluorescent UV Exposure of Plastics 1, ASTM international, West Conshohocken, PA, 2000. www.astm.org.
[24] M. Rice, T. Ramotowski, Activation energy calculations for the diffusion of water into PR-1590 and pellethane 2103-80AE polyurethanes, NUWC-NPT Technical Memo 11-062, 2011.
[25] ASTM D570-80, Standard Test Method for Water Absorption of Plastics 1, ASTM international, West Conshohocken, PA, 2019. www.astm.org.
[26] J. Crank, The Mathematics of Diffusion UK, second ed., Oxford University Press, 1975. ISBN-13: 978-019853411.
[27] T.M. Aminabhavi, R.W. Thomas, P.E. Cassidy, Predicting water diffusivity in elastomers, Polym. Eng. Sci. 18 (1984) 1417–1420. https://onlinelibrary.wiley.com/doi/abs/10.1002/pen.760241808.
[28] S.A. Arrhenius, Über die Dissociationswärme und den Einfluß der Temperatur auf den Dissociationsgrad der Elektrolyte, Z. Phys. Chem. 4 (1889) 96–116, https://doi.org/10.1515/2Fzpch-1889-0408.
[29] W. Chen, B. Zhang, M.J. Forrestal, A split Hopkinson bar technique for low-impedance materials, Exp. Mech. 39 (1999) 81–85.
[30] N. Fredj, S. Cohendoz, S. Mallarino, X. Feaugas, S. Touzain, Evidencing antagonist effects of water uptake and leaching processes in marine organic coatings by gravimetry and EIS, Prog. Org. Coating 67 (2010) 287–295, https://doi.org/10.1016/j.porgcoat.2009.11.001.